

# A Study of Al<sub>2</sub>O<sub>3</sub>-metal composite coatings fabricated by SHS melting-casting

Yaqun Hu<sup>1,a</sup>, Zehua Zhou<sup>1</sup>, Zehua Wang<sup>1</sup>, Ming Xia<sup>1</sup>, Huan Sheng<sup>1</sup>

<sup>1</sup>College of Mechanics and Materials, Hohai University, Nanjing, 210098, China

<sup>a</sup>email: yaqun1989217@163.com

**Keywords:** Al<sub>2</sub>O<sub>3</sub>-metal coating; Melting-casting; Interface bonding; Microstructure

**Abstract.** Al<sub>2</sub>O<sub>3</sub>-metal composite coatings were successfully prepared on carbon steel substrate by self-propagating high-temperature synthesis (SHS) melting-casting means. The effects of transition layers of a bi-layered structure on the interface combination status of the coating were studied in detail, including the microstructure and the elements distribution in the coating. The results show that the coating has an excellent bonding between the substrate and the coating when the content of Al-MoO<sub>3</sub> system in the pre-coated transition layer is 30%. Besides, the coating is dense and there is a phenomenon of elements diffusion at the interface.

## 1 Introduction

With the rapid development of modern industry, many metal components of mechanical equipment can be in adverse long-term use of working conditions. And wear is one of the main failure forms. It cannot be ignored that wear leads to enormous and unavoidable economic loss. Thus, improving wear resistance of key components is a feasible way to prolong the service life of the equipment. We need to improve wear resistance of the material surface. However, it is difficult to meet the engineering requirements using pure metal materials now. Fabricating composite ceramic coatings on metal surface is a very effective method which make materials not only keep the metal strength and toughness, but also receive unique properties of ceramics such as excellent wear resistance, good corrosion resistance and thermal resistance [1-2].

At present there are many preparation methods of ceramic coating, including thermal spray [3-4], vapour deposition method [5-6], sol-gel method [7], laser cladding [8], plasma cladding [9] and self-propagating high-temperature synthesis (SHS) [10].

Compared with other coating technologies, SHS method owns the following advantages [11-13]: no complex manufacturing process and expensive equipment are required; synthetic product is high purity; the reaction duration is rapid; there is high production efficiency; energy consumption is vastly reduced; etc. As a simple method and relatively novel for manufacturing certain ceramic coating, this method has received considerable attention.

In this study, we have designed a bi-layered structure of pre-coated coating to prepare Al<sub>2</sub>O<sub>3</sub>-metal composite coating on steel substrate using SHS melt-casting under an atmospheric environment. The interface combination status, microstructure and the elements distribution of the coating were investigated.

## 2 Experimental

### 2.1 Fabrication of the SHS coating

Detailed summary of the characteristics of the various reactant powders are given in Table 1.

Table 1 Properties of the reactant powders

| Powder        | Fe <sub>2</sub> O <sub>3</sub> | Cr <sub>2</sub> O <sub>3</sub> | NiO   | MoO <sub>3</sub> | Al      |
|---------------|--------------------------------|--------------------------------|-------|------------------|---------|
| Purity (wt%)  | 99.0                           | 99.0                           | 98.0  | 99.5             | 99.0    |
| Particle size | 0.2-0.8 μm                     | 0.5-2.0 μm                     | <50nm | —                | 4-70 μm |

The raw powders of the SHS system were based on the chemical reactions shown in Eqs.(1)-(4)

respectively. Considering the easy oxidation of aluminum powder, a little more Al powders were added to ensure the reaction of  $\text{Fe}_2\text{O}_3$  and  $\text{Cr}_2\text{O}_3$  proceed completely. So the molar ratio of  $\text{Fe}_2\text{O}_3:\text{Cr}_2\text{O}_3:\text{Al}$  was fixed at 6:4:21 and the pre-coated layer of Al- $\text{Fe}_2\text{O}_3$ - $\text{Cr}_2\text{O}_3$  system was regarded as working layers. The molar ratio of NiO:Al and  $\text{MoO}_3:\text{Al}$  was depended on the reaction formulas (3) and (4). The other pre-coated layer of Al-NiO system and Al- $\text{MoO}_3$  system were designed for



transition layers. Our previous study indicated that the coating produced by the single transition layer of Al- $\text{MoO}_3$  system spattered excessively and the porosity of the coating was very high. Al- $\text{MoO}_3$  system and Al-NiO system which has lower reaction heat, good wettability can be made up a hybrid system. Table 2 exhibits the different mixing ratios of the transition layer and the serial number of the produced coating.

Table 2 Parameters of different samples

| Sample                   | Coating 1 | Coating 2 | Coating 3 | Coating 4 |
|--------------------------|-----------|-----------|-----------|-----------|
| Al- $\text{MoO}_3$ (wt%) | 10%       | 20%       | 30%       | 40%       |

These raw material powders were dry-mixed for 6 h by a ball-mixing mill and homogeneous mixture of the reactants can be obtained. Selected carbon steel Q235 which was machined to the size of 50mm×40mm×6mm as the substrate. Before coating, the surface of the substrate was polished and cleaned. The working layer and the transition layer were mixed to a paste with alcohol in the mixer. Then deposit the transition layer paste on the substrate with a thickness of approximately 2mm. Then the coated sample was dried in an oven for 2h at 100 °C. The working layer paste was deposited above the transition layer and the thickness was about 15mm. After 6 hours take the sample out from the oven. Then preheat the assembled sample to 500°C in a resistance furnace. Eventually the reactant powders were ignited with considerable heat released by the magnesium ribbon combustion.

## 2.2 Coating Characterization

The microstructure and the coating morphology, the interface area of the surface and the coating were observed with the Olympus optical microscope (OM, OLYMPUS BX51M, Japan) and scanning electron microscope (SEM, HITACHI S-3400N, Japan). Elements distribution was determined by using X-ray energy-dispersive spectroscope (EDS, HORIBA EX-250, Japan).

## 3 Results and Discussion

### 3.1 Morphology of the interface region

SEM images of interface of the coatings are exhibited in Fig.1. Some large cracks can be seen at the interface of the coating 1 (Fig.1a). With the content increasing of Al- $\text{MoO}_3$  system in pre-coated transition layer, the interface bonding quality of the coating was improved. It can be seen obviously that the cracks decrease and even disappear at some interfacial region of coating 2 (Fig.1b) and coating 3 (Fig.1c). This can be attributed to the large reaction heat during the SHS process. High temperature makes the slight molten area of substrate surfaces increase which is benefited to the combination of the coating with the substrate. With the Al- $\text{MoO}_3$  system content increasing to 40%, the transition layer has a drastic reaction which leads to the products splashing seriously. As a result, the coating obtained is not integrated. Fig.1(d) shows the diffusion of Fe, Al, Cr, and Mo at the interface region coating 3. And the Mo elements which have a better wettability with metallic and ceramic assemble at the interface. The formation of metallurgical bonding between the coating and the substrate can be seen in Fig.1(d) as well. However, Ni elements were not found in EDS. Maybe the reason is that Fe and Ni can form infinite solid solution, therefore, Ni formed some larger metal particles with Fe which was produced by the SHS reaction in certain areas of the interface.

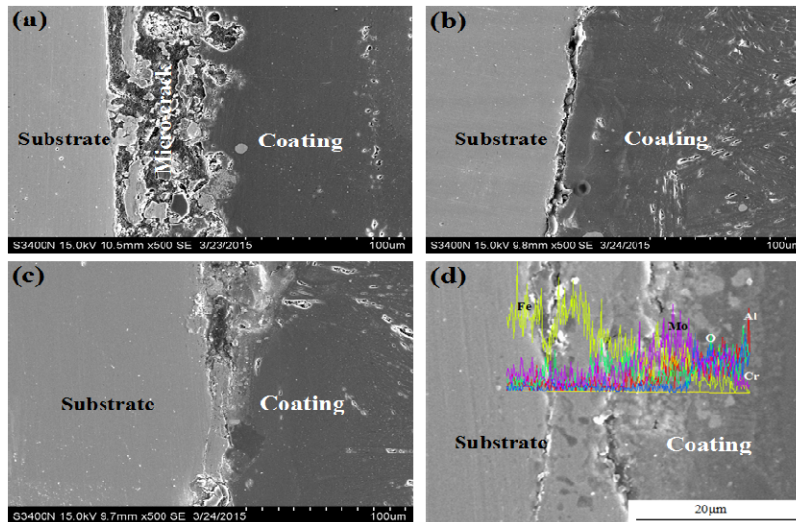


Fig 1. Interface images of coatings with coating 1(a), coating 2(b), coating 3(a) from SEM and EDS analysis at the interface of coating 3(d).

### 3.2 Microstructure and Elements Distribution in the coating

SEM photograph of the central area of the coating 3 is shown in Fig.2. It is notable that the coating near the interface was very dense with few small pores. And there are a bit of metal particles distributed irregularly in the coating. Pores are dependent on the increase of the distance of the interface of the coating. As a result, the pores grow in number and size. Simultaneously we could observe that the columnar crystals grow perpendicular to the interface. However, the structure begins to grow promiscuously when crystals reached to a certain degree. Because of the process cool rapidly which is a non-equilibrium, drastic reaction will make the heat flow in a mess. As a result, the columnar crystal not all grow along vertical direction of the steel substrate, but the columnar crystals are certain to grow parallel to each other.

Fig.3 shows the scanning electronic microscopy photograph of the top area of coating 3. Columnar structure becomes more bulky as it is observed from Fig.3. Owing to the effect of a large undercooling on grain refinement the solidification structure is small and dense near the interface. However, with slower cooling rate the

grain of the upper coating grows during solidification. Besides the adjacent structure which combined closely is an obvious composition segregation. As is shown in Table 2, the elements content of Al and O in the area B is lower than that in the area A. In opposite to Al and O, the elements content of Cr is higher in the area A. According to the spectrum of EDS, it can be found that the elements content of Cr reaches 37% where massive microstructure come into being. There are bright spots placed randomly in columnar structure from the SEM photograph. These spots are a form of solid solution which is composed of the remaining elements of chromium and iron tested by EDS analyzing. Considering of data in the Table 2 and XRD patterns,  $Al_2O_3$  was the primary component of columnar structure.

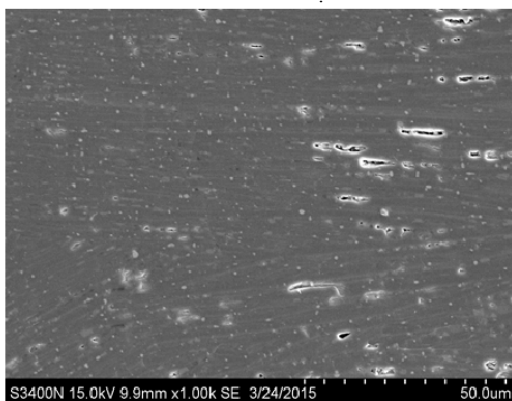


Fig.2 SEM photograph of the central area of coating 3

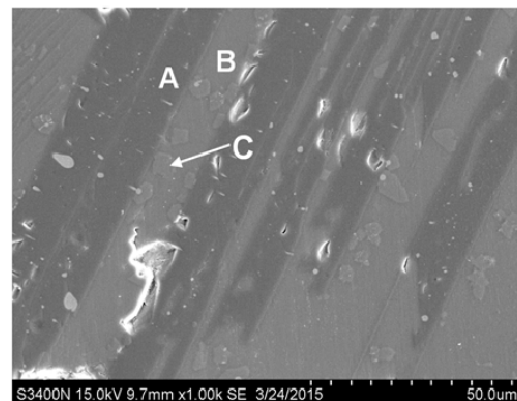


Fig.3 SEM photograph of the top area of coating 3

Table 2 EDS analyze of points A B C in Fig.3

| Elements | A     |       | B     |       | C     |       |
|----------|-------|-------|-------|-------|-------|-------|
|          | mass% | at%   | mass% | at%   | mass% | at%   |
| O        | 53.88 | 67.38 | 37.56 | 51.45 | 35.57 | 56.38 |
| Al       | 41.67 | 30.90 | 56.91 | 46.22 | 27.00 | 25.38 |
| Cr       | 4.46  | 1.72  | 5.54  | 2.33  | 37.42 | 18.25 |

#### 4 Conclusion

Al<sub>2</sub>O<sub>3</sub>-metal composite coating on the carbon steel substrate was successfully fabricated by the means of SHS melting-casting. The coating with the pre-coated transition layer of 30wt.% Al-MoO<sub>3</sub> system was easier to obtain a dense microstructure and metallurgical bonding in certain areas. There was a phenomenon of element diffusion region at the interface between the coating and the surface. Moreover, columnar grain structure was obvious in coating 3.

#### Acknowledgments

This work is supported financially by the National Nature Science Foundation of China (Grant No.51379070).

#### References

- [1] Leivo E M, Vippola M S, Sorsa P P A, et al. Wear and corrosion properties of plasma sprayed Al<sub>2</sub>O<sub>3</sub> and Cr<sub>2</sub>O<sub>3</sub> coatings sealed by aluminum phosphates[J]. Journal of Thermal spray technology, 1997, 6(2): 205-210.
- [2] Shi L, Sun C, Gao P, et al. Mechanical properties and wear and corrosion resistance of electrodeposited Ni-Co/SiC nanocomposite coating[J]. Applied Surface Science, 2006, 252(10): 3591-3599.
- [3] Wang Y, Tian W, Yang Y. Thermal shock behavior of nanostructured and conventional Al<sub>2</sub>O<sub>3</sub>/13 wt% TiO<sub>2</sub> coatings fabricated by plasma spraying[J]. Surface and Coatings Technology, 2007, 201(18): 7746-7754.
- [4] Zhang J, Wang Z, Lin P, et al. Effect of Sealing Treatment on Corrosion Resistance of Plasma-Sprayed NiCrAl/Cr<sub>2</sub>O<sub>3</sub>-8wt.% TiO<sub>2</sub> Coating[J]. Journal of thermal spray technology, 2011, 20(3): 508-513.
- [5] Jeong Y H, Choe H C, Eun S W. Hydroxyapatite coating on the Ti-35Nb-xZr alloy by electron beam-physical vapor deposition[J]. Thin Solid Films, 2011, 519(20): 7050-7056.
- [6] Wang X, Feng H, Wu Y, et al. Controlled synthesis of highly crystalline MoS<sub>2</sub> flakes by chemical vapor deposition[J]. Journal of the American Chemical Society, 2013, 135(14): 5304-5307.
- [7] Tiwari S K, Sahu R K, Pramanick A K, et al. Development of conversion coating on mild steel prior to sol gel nanostructured Al<sub>2</sub>O<sub>3</sub> coating for enhancement of corrosion resistance[J]. Surface and Coatings Technology, 2011, 205(21): 4960- 4967.
- [8] Masanta M, Ganesh P, Kaul R, et al. Development of a hard nano-structured multi-component ceramic coating by laser cladding[J]. Materials Science and Engineering: A, 2009, 508(1-2): 134-140.
- [9] Lu J B, Meng P, Tang F, et al. Microstructure Analysis of TiC Reinforced Fe-Based Composite Coating by Plasma Cladding[J]. Advanced Materials Research, 2012, 472: 297-301.
- [10] Miao S, Puszynsla J A. The effect of additives on microstructure and phase separation of SHS-densified materials[J]. Inter JSHS, 1998, 7: 349-360.
- [11] Varma A, Lebrat J P. Combustion synthesis of advanced materials[J]. Chemical Engineering Science, 1992, 47(9): 2179-2194.
- [12] Merzhanov A G. The chemistry of self-propagating high-temperature synthesis[J]. Journal of

Materials Chemistry, 2004, 14(12): 1779-1786.

[13] Tjong S C, Ma Z Y. Microstructural and mechanical characteristics of in situ metal matrix composites[J]. Materials Science and Engineering: R: Reports, 2000, 29(3): 49-113.